Fibers and Polymers 2020, Vol.21, No.4, 821-828
DOI 10.1007/s12221-020-9600-x

ISSN 1229-9197 (print version)
ISSN 1875-0052 (electronic version)

Experimental and Numerical Study of the Critical Length of Short Kenaf Fiber Reinforced Polypropylene Composites

Mohammad Nematollahi[1]*, Mehdi Karevan[2], Marzieh Fallah[2], and Mahmoud Farzin[2]

[1]*Department of Biosystems Engineering, University of Manitoba, Winnipeg, MB R3T 5V6, Canada*
[2]*Department of Mechanical Engineering, Isfahan University of Technology, Isfahan 8415683111, Iran*
(Received June 10, 2019; Accepted September 10, 2019)

Abstract: Widespread attention to make use of biodegradable resources as a replacement for petroleum products leads to the exploitation of natural fiber reinforced composites. Natural fiber reinforced polymer composites usually exhibit lower mechanical properties than synthetic fiber ones. Thus, understanding key factors affecting the overall mechanical properties in order to increase them is crucial. One underlying factor is the length of fiber highly contributing to the extent of matrix/ fiber interfacial load transfer at the interface. However, the concurrent examination of the load transfer mechanism at the interface of fiber/matrix in terms of fiber length has not been well performed using computational, analytical and experimental approaches. This work is aimed at the determination of the critical fiber length associated with a full load transfer condition using various methods to better understand their accuracy and the interfacial load transfer mechanism. For this purpose, specimens of neat polypropylene (PP) and 20 wt% kenaf/PP composites were fabricated using extrusion injection molding. Tensile testing, scanning electron microscopy and density measurements were conducted to incorporate the obtained results into the models and to verify the results predicted by the models. A three dimensional representative volume element (RVE) representing the filler content of fabricated specimens was assumed. A micromechanical model was employed to make the results of analysis independent of the RVE dimensions. The critical fiber length for a full load transfer was determined by evaluating the stored elastic strain energy changes against the fiber length. The results showed that the kenaf fiber length is critical to both the load transfer efficiency and stiffening of composites. The results further revealed that to obtain the full interfacial load transfer, the length of kenaf fibers needs to be greater than the critical length being ~2.4 mm provided that perfect kenaf/PP interfacial interaction exists.

Keywords: Composites, Load transfer, Melt mixing, Critical fiber length, FEM

Introduction

Short fibers have been used as the reinforced phase for polymers to specially improve their mechanical performance. Recently, the use of natural fibers as a substitute for man-made fibers in polymer composites has been widely increased [1]. Natural fiber composites have a wide range of advantages than synthetic fiber composites such as their low cost, low density and environmentally friendly properties [2]. However, the overall mechanical properties of synthetic fiber composites are greater than natural fiber based composites [3].

A large number of factors affect the overall mechanical properties of composites, most important of which include fiber type, matrix type, the fiber loading, the manufacturing process, the interface formed between reinforcement and matrix phase, and the length of fibers. In natural fiber composites, it is evident that increasing the amount of fibers, up to an optimum, leads to the increase in mechanical properties in particular tensile and flexural properties [4]. The fabrication process of composites has a direct effect on their properties and dramatically dictates the quality of fibers dispersion in matrix. Common methods such as hot press, extrusion, and injection molding have been largely reported in the processing of natural fiber reinforced polymers [5]. However, less research has scrutinized on the correlations between the techniques used in association with the length of fibers and overall bulk properties. It is largely accepted that one key factor directly related to the length of fibers is the processing itself [6].

The quality of interface formed at matrix and fiber surface is another critical issue tremendously affecting the mechanical properties of composites even though in there exists weak compatibility between fibers and the matrix natural fiber composites, in particular, when fibers are mixed with non-polar polymers [7]. Some methods are used to overcome this issue such as the use of chemical treatment that in turn provides a better adhesion at the fiber and matrix interface and incorporation of a coupling agent to enhance the degree of fiber and matrix adhesion [8]. Nishino *et al*. [9] used X-ray diffraction to investigate the load transfer at the composites interface, kenaf fibers and poly-L-lactic acid (PLLA) resin. It was shown that when silane was used in the treatment of kenaf fibers, stronger adhesion and interfacial interaction at the interface of matrix and fiber are created and a better stress transfer is provided from the matrix to kenaf fibers. It should be noted that the effect of interface on the load transfer from matrix to the fiber is even more critical in the case of nanocomposites due to their higher aspect ratio of nano reinforcements than micro-scale fillers in the case of traditional micro composites [10,11].

The length of fibers has a significant role in mechanical

*Corresponding author: nematolm@myumanitoba.ca

properties of composites because a full load transfer between the matrix and fiber occurs when the fiber length is more than the critical fiber length [12]. Numerous studies have investigated the role of fiber length in the load transfer mechanism of fiber reinforced composites [13-15]. Migneault *et al*. [15] found that the increasing fiber length dramatically affects the tensile, flexural, and toughness of wood polymer composites. Various theoretical models and finite element methods have been utilized to explore the relationship between the fiber length and mechanical properties of composites. Fu *et al*. [16] modelled the fiber length to use it for predicting the elastic properties of short fiber composites. They found that the strength of composites improved when the fiber length was near the critical fiber length and for the length of fiber which was five times more than the critical fiber length, the strength of composites approached a plateau level. Shalwan *et al*. [17] reported that the decrease of fiber length more than the critical length caused the decrease of stress transfer efficiency between the matrix and the fiber.

In this paper, we focused on the understanding of the region of critical fiber length and calculated this length from the FEM method. To do this, an analytical solution was used to determine the RVE dimensions with respect to varying aspect ratio of fibers. For sake of comparison, kenaf/PP composites were fabricated using extrusion injection molded method and the length of fibers were obtained in order to verify the FEM results. The results of the current study are further useful in exploring the relationships among fabrication process, microstructure and bulk properties of fiber reinforced composites when processing technique is to be taken into account in the modeling or prediction of overall mechanical properties of fabricated composites.

Experimental

Materials

Kenaf fibers were imported and purchased from Malaysia. The length of fiber was equal to 2 meters for each bundle. Polypropylene, (PP), homopolymer type (melt flow index 29.1 g/10 min, isotactic >90 %), was purchased from Hyosung Company, South Korea. Maleic Anhydride Polypropylene, (MAPP), (melt flow index 110 g/10 min), was used as a coupling agent for improving adhesion of kenaf fibers to the polypropylene substratum and purchased from Exxon Mobil Company, USA. Moreover, sodium hydroxide, (NaOH) was used in order to modify the surface of the short kenaf fibers. This material also was purchased from DLM Company, Germany, with purity of 99.99 %.

Fabrication of Composites

To prepare the composite specimens, dried fibers, PP granules and coupling agent were melt mixed. The specimens contain 20 wt% kenaf fibers and 2 % MAPP into the PP matrix. The prepared compounds were melt mixed by an industrial twin-screw extruder, Dr. Collins GmbH, Germany, with the L/D of 16 including five different heating at 40 rpm and the barrel temperature range of 170-190 °C from the feeding zone to the die zone, respectively. The extruded compound was then cut into long strands and hot air blown for drying. The prepared strands were cut into the small composite pellets for facilitating the molding process. The pellets were placed in a vacuum oven at 100 °C for 3 hours to remove the moisture content before the injection process. The composite specimens were fabricated using a closed molding injection machine, (HAIXING Company, China, with the capacity of 88 tons clamping force and injection capacity of 111 grams of polystyrene) with the barrel temperature 170 to 195 °C. The mold temperature of 40 °C and freezing time of 20 s were used for the injection process. Figure 1 shows the specimens fabricated by injection molding method. It should be mentioned that in this work, kenaf fibers were first chemically treated to eliminate any other impurities. The kenaf fibers were cut into small length being around 10 mm. For the chemical modification of kenaf short fibers, the fibers were soaked into NaOH solution. To achieve this, a solution with 5 % NaOH and soaking times of 3 hr were prepared. Therefore, the kenaf fibers were first soaked in NaOH solution at specific duration of soaking time. The fibers then were put in distilled water for 24 hours, and then removed and washed with distilled water for the last time. The fillers were dried for 24 h in a vacuum oven at 80 °C to remove its moisture.

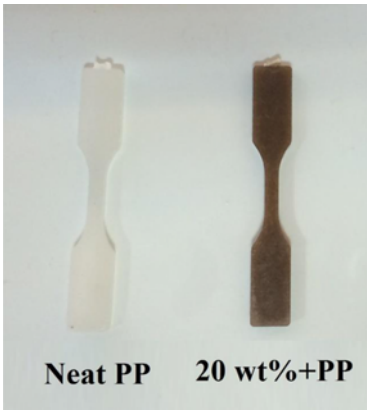

Figure 1. Neat PP and 20 wt% kenaf fiber reinforced PP composites specimens for tensile test.

Characterization

The scanning electron microscope (SEM), XL30, Philips Co, Netherlands, was utilized to study the morphology and the surface of kenaf fibers before and after chemical treatment. The tensile behavior of fibers was conducted after their chemical treatment and fibers were prepared according to ASTM C1557. A universal testing machine (Zwick, 1,446-60) with gauge length of 30, 50, and 70 mm and the

0.05 mm/s cross-head speed, was used to perform the tests of fibers. The test was carried out for 15 fibers to determine tensile properties and system compliance as well. The tensile behavior of the specimens was characterized using a tensile analyzer (STM-50, Santam Company) according to ASTM D638 standard at a cross head speed of 5 mm/min. It should be mentioned that to ensure the integrity of the results, 5 specimens were prepared under the same condition for characterization. To find the density of the PP and fiber, a gas pycnometer (Quantachrome; USA, model- MVP - 5 DC) was used and 10 samples of treated kenaf fibers and PP granules using helium gas at 25±2 °C were tested to give an averaged value.

Fiber Length Distribution

To find the length of the fiber after injection, the composite specimens were placed into the xylene solution as a good solvent for polypropylene. To do this, the samples were boiled at 150 °C for 2 hours to solve the polypropylene and to extract short kenaf fibers after solving their neighboring polymer. Then, the fibers were laid on a microscope glass slide and optical microscope, EPIPHOT 300, Nikon Co. USA, was used to estimate the kenaf fibers length by direct measurement of the micrographs with ImageJ software. Numerous fiber residuals of composites were analyzed and recorded.

Computational

Generation of 3D RVE

For a better understanding of the effect of fiber length in the reinforcing efficient and role of the critical length of fibers in mechanical response of kenaf/PP composites a computational approach was adopted. It has been widely shown that square or cubic RVEs are employed in numerical modeling approached since such geometries facilitate solutions in problem associated with numerical boundary values. An accurate determination of RVE sizes is so challenging because of the difficulties involved in generating statistical information about particle distributions and concentrations [18], besides the dimensions of the RVE extremely affect the results especially longitudinal Young's modulus. Consequently, the selection of correct RVE sizes that determine exact properties of composites is completely necessary. In this study, to find the correct dimensions of RVE, the Halpin-Tsai micromechanical model and the analytical solution were developed. The same method has been used in elsewhere [19,20]. Qian *et al*. [21] showed that Halpin-Tsai model and their experimental results had a decent adaptation with each other. Also, supported that there was a good agreement between the results of Halpin-Tsai model and FEM model.

Analytical Solution

To develop the formula for analytical solution, one-eighth of the RVE was considered as is represented in Figure 2. The symmetrical geometry and the loading conditions were divided into three parts. Part 1 is the polymer at the end of the RVE, part 2 is the fiber that is embedded within the RVE and part 3 is the polymer surrounding the fiber. The length of the RVE that is parallel with the fiber length and another dimension of the RVE which is the diameter of cylindrical cross-sectional are named a and b, respectively.

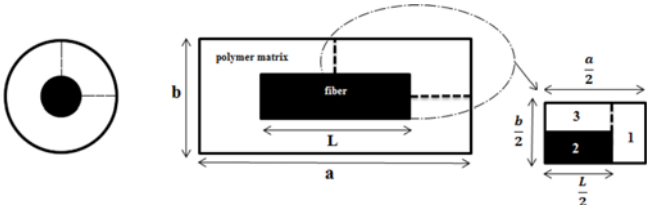

Figure 2. Representative volume element of composites showing the fiber embedded in matrix as well as representing component boundaries.

The spring constant (K) of each part along the fiber length is determined by the following equation:

$$K = \frac{AE}{L} \tag{1}$$

where A, E, and L are area, Young's modulus and length of each part, respectively. According to the combination rules of spring, part 2 and 3 are parallel springs and the equivalent of the said system is series with part 1. Thus, by writing the equations between spring constants and simplifying them, the following equation is resulted to determine the longitudinal Young's modulus of the RVE:

$$E_{11} = \frac{1}{\dfrac{a - L_f}{aE_p} + \dfrac{4L_f b^2}{4E_p ab^2 + \pi {d_f}^2 a(E_f - E_p)}} \tag{2}$$

Halpin-Tsai Micromechanical Solution

The Halpin-Tsai equation for the calculation of the elastic modulus of short fiber reinforced composites was employed as given below [22]:

$$E_c = \frac{3}{8}E_{11} + \frac{5}{8}E_{22} \tag{3}$$

where E_{11} and E_{22} are the longitudinal and transverse modulus, respectively, which are given as followed:

$$E_{11} = \frac{1 + 2(L_f/d_f)\eta_L V_f}{1 - \eta_L V_f}E_p \tag{4}$$

$$E_{22} = \frac{1 + 2\eta_T V_f}{1 - \eta_T V_f}E_p \tag{5}$$

where η_L and η_T are given by the following phrases:

$$\eta_L = \frac{(E_f/E_p)-1}{(E_f/E_p)+2(L_f/d_f)} \quad (6)$$

$$\eta_T = \frac{(E_f/E_p)-1}{(E_f/E_p)+2} \quad (7)$$

where L_f, d_f, V_f, E_f, and E_p are fiber length, fiber diameter, volume fraction of fiber, elastic modulus of fiber, and elastic modulus of polymer, respectively.

By equating equations (2) and (4), we can achieve one equation between two parameters a and b. Besides, a constant volume fraction of the fiber gives another equation between a and b as mentioned below:

$$vol_f\% = \frac{wt_f\%}{wt_f\% + (1-wt_f\%)\frac{\rho_f}{\rho_p}} = \frac{vol_f}{vol_f + vol_p} = \frac{\frac{\pi d_f^2}{4}L_f}{a^2 b} \quad (8)$$

In this equation, wt%, ρ_f, ρ_p, vol_f, and vol_p are the weight fraction of fiber, the density of fiber, the density of polymer, the volume fraction of fiber, and the volume fraction of polymer, respectively.

The Finite Element Model

A 3D one-eighth model of RVE consisting of the kenaf fiber embedded in the polymer matrix is analyzed by a finite element model in Abaqus 6.14 (Dassault system). To this aim, fibers are distributed uniformly in the matrix phase, and both matrix as well as fiber are assumed to be homogeneous and linearly elastic. Additionally, a perfect bonding at the interface of fiber/matrix is considered [18,23]. In the model, the boundary z=0 is fixed in the axial direction and free to move in the lateral directions. Moreover, two symmetric boundary conditions are supposed for x=0 and y=0 planes as well as a uniform force applied on the z=l surface. It should be noted that the dimensions and material properties of the fiber and matrix used in this method are mostly obtained from current experiment describing in the following.

Evaluation of Strain-energy-change

Under certain loading conditions, when a stiff fiber embedded into a soft polymer matrix, the strain energy of polymer decreases. Based on various micromechanics models, the Evaluation of strain-energy-changes for different fiber lengths is essential to calculating the critical fiber length [24]. The strain-energy for the pure polymer matrix as a cube with dimensions a and b is determined analytically by the following calculation:

$$U_p = \frac{\sigma^2}{2E_p}V_m = \frac{\sigma^2}{2E_p}ab^2 \quad (9)$$

where E_p, E_m and σ are Young's modulus of polymer, the volume of matrix, and far field stress respectively. One may subtract equation (9) from the FEM results obtained to determine the changes in the strain energy against the variation in the fiber length. Finally, it should be mentioned that for validation of the FEM results, experimental values will be incorporated. The Young's modulus of composites obtained from experimental and FEM results with the same aspect ratio was then compared to verify of the validity of the model used.

Results and Discussion

Scanning Electron Microscope of Fibers

The SEM observations were performed to study the morphology of the fiber surface before and after the chemical treatment following the steps mentioned earlier. Figure 3(a) displays the SEM micrographs obtained from the surface of unmodified kenaf fibers. As is seen in Figure 3(a), the surface of the fibers contains impurities and contamination that need to be eliminated by chemical treatment to provide a stronger adhesion at the kenaf/PP interface. The thick and compact structure of unmodified fibers indicates that the cellulose fibers are connected to lignin and pectin molecules. Figure 3(b) is a representative image of a modified kenaf surface using 5 % NaOH with 3 hr treatment time. As is shown in Figure 3(b), the surface of kenaf fibers has no significant impurities and becomes thin with a rough surface. This finding could be thought of the presence of surface modified fibers as a result of the removal of non-cellulosic components (lignin and pectin) as well as components with low molecular weight. The elimination of impurities from kenaf fiber structure improves the adhesive properties of fiber surface leading to significant improvement

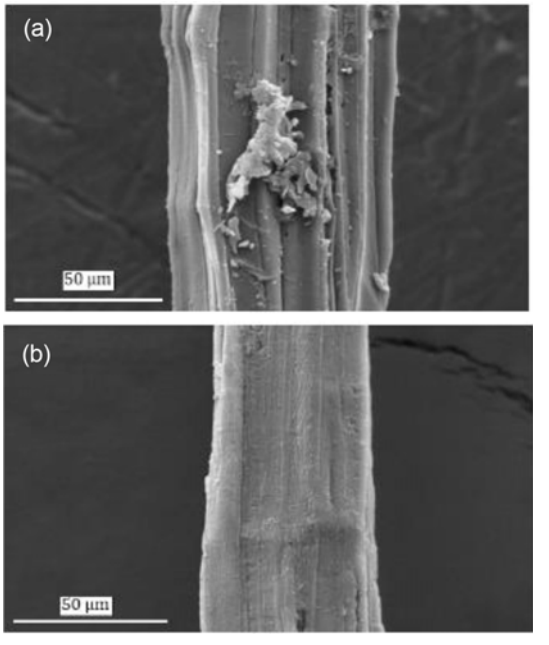

Figure 3. SEM image of (a) unmodified kenaf fibers, kenaf fibers modified with (b) 5 % NaOH during 3 hr soaking time.

in mechanical properties due to the strong bonding of cellulose fibers and polymer matrix as frequently reported elsewhere [25]. In addition, it is easily shown that the average diameter of the modified kenaf fibers is around 60 μm.

Mechanical Properties of Fibers and Composites

Figure 4 presents setup of the tensile test, universal testing and machine detail of clamps and specimen, and the tensile behavior of a kenaf fiber. The Young's modulus of kenaf fibers was calculated in its elastic portion of the stress-strain curve. The kenaf fiber presents the Young's modulus of about 40 GPa. As it was mentioned before, this result corresponds to the kenaf fibers that was treated by 5 % NaOH with soaking time of 3 hr.

Figure 5 illustrates comparative average force-extension curves for tensile tests of neat pp and PP/kenaf composites reinforced with 20 wt% of kenaf for five specimens. As it is evident from the figure, the tensile modulus of the specimens considerably increases with the increase in the kenaf content and the addition of 20 wt% kenaf fibers to the PP+MAPP matrix results in a 100 % increase in the tensile modulus of the composites compared to that observed in the case of neat PP. Young's modulus of neat PP and PP/kenaf composites that are obtained from the tensile test is 1 and

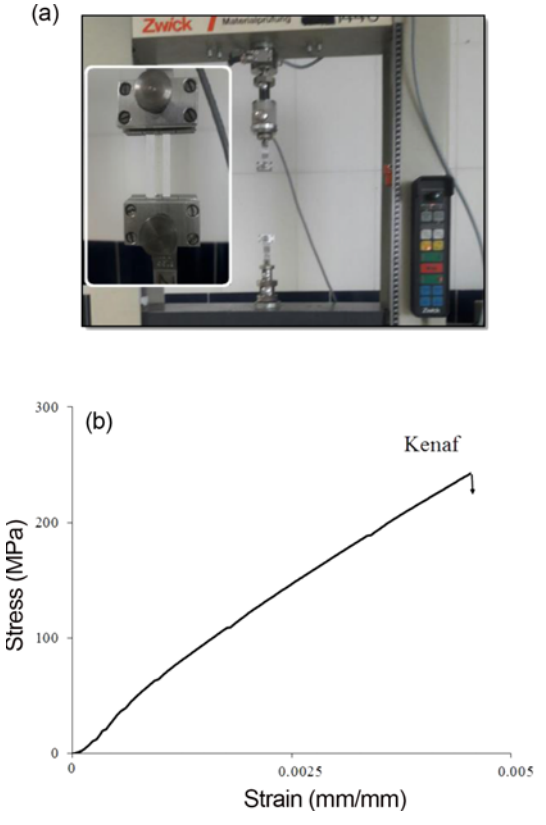

Figure 4. (a) Setup of the tensile test according to ASTM C155 and (b) stress-strain behavior of a kenaf fiber.

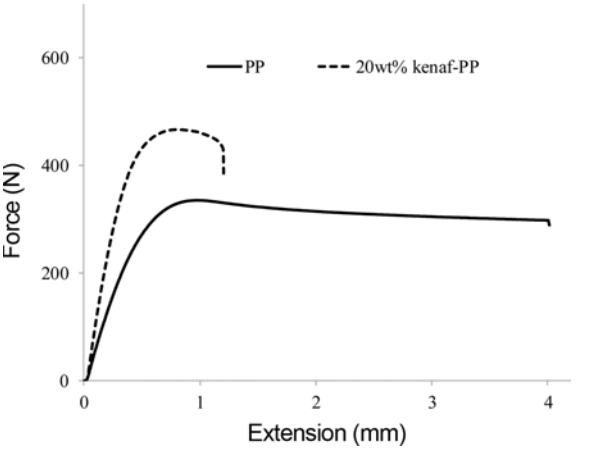

Figure 5. Force-displacement for neat PP and 20 wt% of kenaf/PP composites obtained from tensile test.

2 GPa, respectively. The reason is that due to the stiffening effect of a harder phase within the matrix, the greater tensile modulus of kenaf fibers is expected to enhance the elastic response of composites.

The Density Measurement of Kenaf Fibers and PP

Measurements obtained from the helium pycnometry test of treated kenaf fibers as well as PP, and the results reveal that the density of treated kenaf fiber and PP is 1.45 gr/cm^3 and 0.855 gr/cm^3, respectively. Thus, dimensions and material properties of the fiber and matrix to use in analytical solution and FEM were calculated and listed in Table 1.

Average Kenaf Fiber Length of Composites

Figure 6 demonstrates the fiber length distribution of kenaf fibers extracted from injection-molded specimens of 20 wt% fiber loading. The average fiber length of kenaf fiber before compounding is around 10 mm. The extracted kenaf fibers exhibit a narrow fiber length distribution with 75 % of fiber length falling in the rage of 0.4-0.8 mm. As shown in Figure 6, the average length of kenaf fiber after the injection process is around 0.6 mm. It is evident that the final fiber lengths of composites are lower than those observed before processing due to the presence of shear forces during the mixing. However, the final length of the fibers are dictated

Table 1. Material properties and geometric characteristics of the phases considered in modeling

Material	Young's modulus (GPa)	Density (gr/cm^3)	Poisson's ratio	Diameter (μm)
Kenaf	40*	1.45*	0.32 [27]	60*
PP	1*	0.855*	0.36 [28]	No need

*Obtained from the current experimental work.

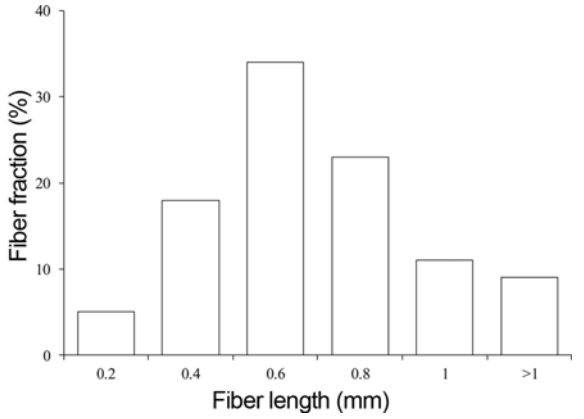

Figure 6. Distribution of the lengths of kenaf fibers within the injected molded PP composites loaded with 20 wt% kenaf fibers and 2 wt% MAPP.

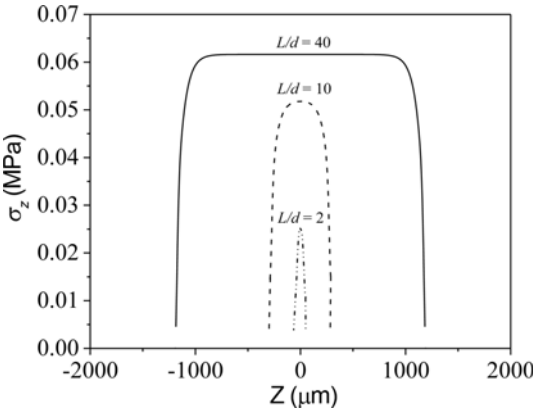

Figure 8. Longitudinal stress distributions along the kenaf fiber for different aspect ratios.

by the processing parameters including the extruder melting zone temperature, fibers residence time in the barrel and screws RPM.

Data Analysis

As was mentioned earlier, the strain energy of matrix changes in the presence of fibers, and these changes could be obtained by subtracting the numerical solution, equation (9), from FEM results. For investigating the effect of different length of fibers on the changes of strain energy, the fiber aspect ratio (L_{fiber}/D_{fiber}) was changed from 2 to 100. Then, the strain-energy-changes were calculated with respect to each fiber aspect ratio. Finally, to obtain the strain-energy-changes per unit length ($\Delta U/L_{fiber}$), the strain-energy-change was divided by the corresponding fiber length.

The variation of $\Delta U/L_{fiber}$ with the aspect ratio of fiber is represented in Figure 7. As Figure 7 shows, when the aspect ratio (L_{fiber}/D_{fiber}) increases, two regions are noticeable. First, the region that $\Delta U/L_{fiber}$ sharply increases followed by a plateau where $\Delta U/L_{fiber}$ gradually converges to a definite value. The stress distribution along the kenaf fiber and this value is closely related to one another. The reason for this observation is attributed to a common theory that the stress distribution could be obtained uniformly in the middle part of the long fibers and also, for very long fibers, the rang of this uniform stress distribution can be extremely larger than the range of non-uniform stress distribution where it was at the ends of fibers (see Figure 8). It is widely accepted that the lower shear strain appearing along the fiber length than that of the two ends is responsible for the observed stress distribution [26]. Consequently, the dominant stresses are in the uniform region and not in non-uniform regions. In this condition, the stresses transferee completely between kenaf fibers and PP matrix. As a result, when the fiber length exceeds the critical length, the strain energy change per unit length reaches a plateau showing that the energy changes per fiber length become constant. It can be easily understood that the lower aspect ratios corresponding to the onset of the plateau region is correlated to the greater reinforcing efficiency of the fibers. The variation in $\Delta U/L_{fiber}$ thus could be well used to quantitatively determine the load transfer quality at the interface of kenaf/matrix.

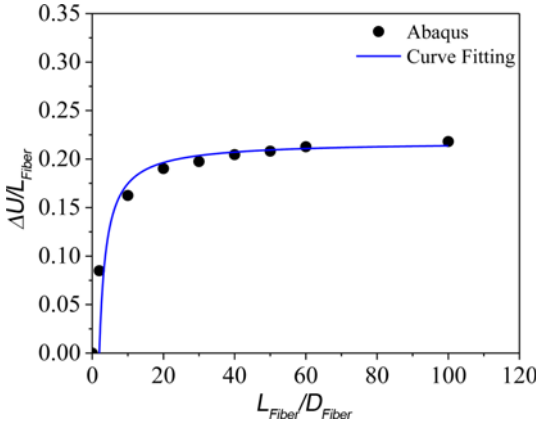

Figure 7. Changing in strain energy per unit fiber length.

According to correlation between the aspect ratio and the energy change per length of fiber described earlier, it was found from Figure 7 that the minimum aspect ratio of kenaf fiber required to provide the full load transfer between kenaf fibers and matrix is 40 and greater above which the value of $\Delta U/L_{fiber}$ gradually converges to a definite value. It means that because the diameter of fiber is 60 μm, the critical length of fiber should be greater than 2.4 mm.

The Young's modulus values obtained from the FEM calculations were validated by experimental results. As shown earlier, the tensile experiments showed a Young's modulus of 2 GPa for the 20 wt% kenaf reinforced specimens. This values was further shown to be corresponded to the aspect ratio of 10 (The average length of kenaf fiber after the injection process was 0.6 mm and the diameter of

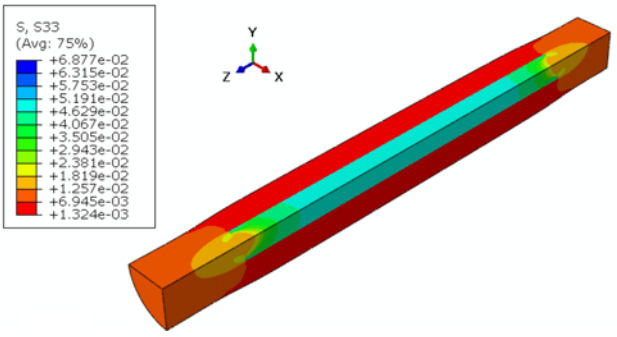

Figure 9. Stress distribution in fiber and matrix for aspect ratio 10.

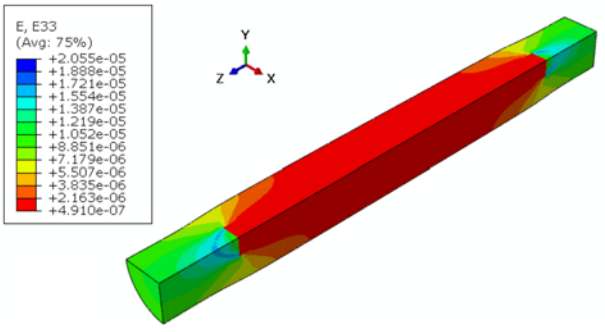

Figure 10. Strain distribution in fiber and matrix for aspect ratio 10.

fibers was 60 μm). To obtain Young's modulus from FEM model, the extensive force has been applied as a tensional force to both sides of RVE to the extent that the composite does not enter the plastic range. Also, the variation in the length of the RVE was obtained from the finite element model and the strain was calculated accordingly. Finally, the Young's modulus can be calculated by dividing the stress by strain. FEM results show the Young's modulus associated with this aspect of ratio is 2.2 GPa being in good agreement with the experimental values. Figure 9 and Figure 10 show the Stress and strain distribution in fiber and matrix for aspect ratio 10 obtained from the FEM method.

Conclusion

In this study, the correlation among elastic properties, fiber length and interfacial load transfer quality was evaluated to better understand of the role fiber length in strengthening of natural fiber reinforced composites. The strain energy changes for different fiber lengths were obtained from the proposed FEM model constructed on the obtained experimental results. The RVE dimensions were calculated with regard to the results of a micromechanical approach to ensure the computational results are independent of the RVE dimensions. The FEM results were validated by experimental data obtained from the mechanical and morphological study of extrusion injection molded specimens. The results indicated that range of critical length of fiber to guarantee the full load transfer between kenaf fibers and PP matrix should be greater than 2.4 mm. Therefore, fibers longer than the critical length are preferable due to their greater reinforcing effects. However, it should be taken into account that fibers of high aspect ratio though theoretically providing better interfacial load transfer might lead to limitations in fabrication of composites due to fiber entanglement, waviness and thus the decrease in eventual properties of fabricated specimens.

Acknowledgments

The authors would like to thank the Nanocomposites and Tissue Engineering Laboratory of the Department of Mechanical Engineering at the Isfahan University of Technology for providing the facilities for performing this study.

References

1. Y. Nawab, M. Kashif, M. A. Asghar, A. Asghar, M. Umair, K. Shaker, and M. Zeeshan, *Appl. Compos. Mater.*, **25**, 747 (2018).
2. A. Oumer and D. Bachtiar, *Fiber. Polym.*, **15**, 334 (2014).
3. P. Wambua, J. Ivens, and I. Verpoest, *Compos. Sci. Technol.*, **63**, 1259 (2003).
4. S. S. Chee, M. Jawaid, M. Sultan, O. Y. Alothman, and L. C. Abdullah, *Compos. Part. B-Eng.*, **163**, 165 (2019).
5. J. A. Silva-Guzmán, R. R. Anda, F. J. Fuentes-Talavera, R. Manríquez-González, and M. G. Lomelí-Ramírez, *Fiber. Polym.*, **19**, 1970 (2018).
6. K. Senthilkumar, N. Saba, N. Rajini, M. Chandrasekar, M. Jawaid, S. Siengchin, and O. Y. Alotman, *Constr. Build. Mater.*, **174**, 713 (2018).
7. S. Biswas, S. Kindo, and A. Patnaik, *Fiber. Polym.*, **12**, 73 (2011).
8. R. Haque, M. Saxena, S. Shit, and P. Asokan, *Fiber. Polym.*, **16**, 146 (2015).
9. T. Nishino, K. Hirao, and M. Kotera, *Compos. Part A. Appl. Sci. Manuf.*, **37**, 2269 (2006).
10. A. Eitan, F. Fisher, R. Andrews, L. Brinson, and L. Schadler, *Compos. Sci. Technol.*, **66**, 1162 (2006).
11. S. Alampalli and J. Kunin, *Appl. Compos. Mater.*, **10**, 85 (2003).
12. P. Amuthakkannan, V. Manikandan, J. W. Jappes, and M. Uthayakumar, *Mater. Phys. Mech.*, **16**, 107 (2013).
13. Y. Feng, Y. Hu, G. Zhao, J. Yin, and W. Jiang, *J. Appl. Polym. Sci.*, **122**, 1564 (2011).
14. H. Takagi and Y. Ichihara, *JSME Int. J. A-Solid. M.*, **47**, 551 (2004).
15. S. Migneault, A. Koubaa, F. Erchiqui, A. Chaala, K. Englund, C. Krause, and M. Wolcott, *J. Appl. Polym. Sci.*,

110, 1085 (2008).
16. S.-Y. Fu and B. Lauke, *Compos. Sci. Technol.*, **56**, 1179 (1996).
17. A. Shalwan and B. Yousif, *Mater. Des.*, **48**, 14 (2013).
18. P. Bhaskar and R. H. Mohamed, *Adv. Mater. Phys. Chem*., **2**, 23 (2012).
19. X. Chen and Y. Liu, *Comput. Mater. Sci.*, **29**, 1 (2004).
20. Y. Liu and X. Chen, *Mech. Mater.*, **35**, 69 (2003).
21. D. Qian, E. Dickey, R. Andrews, and T. Rantell, *Appl. Phys. Lett.*, **76**, 2868 (2000).
22. V. Srivastava and S. Singh, *Int. J. Compos. Mater.*, **2**, 1 (2012).
23. M. A. Bhuiyan, R. V. Pucha, J. Worthy, M. Karevan, and K. Kalaitzidou, *Compos. Struct.*, **95**, 80 (2013).
24. L. Shen and J. Li, *Int. J. Solids Struct.*, **40**, 1393 (2003).
25. P. Phitsuwan, K. Sakka, and K. Ratanakhanokchai, *Bioresour. Technol.*, **218**, 247 (2016).
26. P. K. Mallick, "Composites Engineering Handbook", CRC Press, 1997.
27. V. Mariselvam and M. Logesh, *Int. J. Appl. Eng. Res*., **10**, 617 (2017).
28. M. A. Bhuiyan, R. V. Pucha, M. Karevan, and K. Kalaitzidou, *Comput. Mater. Sci.*, **50**, 2347 (2011).